IEICE Proceeding Series

Analytical Derivation of Switching-pattern Distribution for Class-E Amplifier Using Bifurcation Theory

Tomoharu Nagashima, Xiuqin Wei, Takuji Kousaka, Hiroo Sekiya

Vol. 1 pp. 687-690
Publication Date: 2014/03/17
Online ISSN: 2188-5079

2012 International Symposium on Nonlinear Theory and its Applications
NOLTA2012, Palma, Majorca, Spain, October 22-26, 2012

Analytical Derivation of Switching-pattern Distribution for Class-E Amplifier Using Bifurcation Theory

Tomoharu Nagashima† , Xiuqin Wei††, Takuji Kousaka†††, and Hiroo Sekiya†

†Graduate School of Advanced Integration Science, Chiba University
1-33, Yayoi-cho, Inage-ku, Chiba, 263-8522 Japan
††Department of Electronics Engineering and Computer Science, Fukuoka University
8-19-1 Nanakuma, Jonan-ku, Fukuoka 814-0180, Japan
†††Faculty of Engineering, Oita University
700 Dannoharu, Oita, 870-1192 Japan
Email: nagashima@chiba-u.jp, xiuqinwei@fukuoka-u.ac.jp, takuji@oita-u.ac.jp, sekiya@faculty.chiba-u.jp

Abstract—This paper presents analytical switching-pattern distributions for the class-E amplifier. The switching patterns are changed via border-collision bifurcation or grazing bifurcation. Therefore, the switching-pattern distribution maps can be obtained for wide parameter region by solving the bifurcation conditions with the analytical steady-state waveform expressions and following the bifurcation curves. By carrying out circuit experiments, we can confirm the validity of the distribution maps.

1. Introduction

The class-E power amplifier [1]-[4] is expected to be useful for many applications, e.g., radio transmitters, switching-mode dc-power supplies, devices for medical applications, and so on. Because of the class-E zero-voltage switching and zero-derivative switching (ZVS/ZDS) conditions, the class-E amplifier can achieve high power-conversion efficiency at high-frequencies.

Since the introduction of the class-E amplifier, many analytical descriptions of this circuit have appeared [1]–[4]. Most of these papers focused on the class-E amplifier satisfying the class-E ZVS/ZDS conditions, which is called "nominal conditions". It is important, however, to comprehend behaviors and performance of the class-E amplifier outside nominal conditions.

Recently, there were several analyses for the class-E amplifier outside the nominal conditions [2]–[4]. Especially, the switch-voltage waveform includes important information because it affects the power-conversion efficiency and the switching noise strongly. For example, it is important and useful to know the ZVS region analytically for achieving the high power-conversion efficiency and the low switching noise. In the class-E amplifier, there are some switching patterns, whose appearance depends on the parameter set. There is, however, no research which shows the switching-pattern distributions in the parameter space.

In this paper, the switching-pattern distributions for the class-E amplifier are derived analytically. It is found that the transition conditions of switching patterns are the same as bifurcation conditions of the border-collision bifurcation or the grazing bifurcation [5]. Therefore, it is possible to obtain the switching-pattern distribution maps by solving the bifurcation conditions with the analytical steady-state waveform equations and following the bifurcation curves.

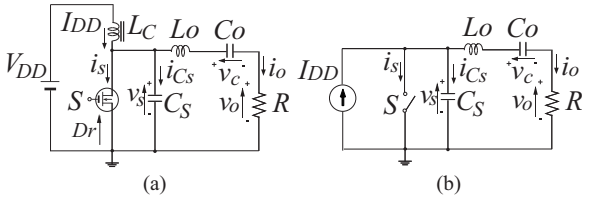

Figure 1: (a) Circuit topology of class-E amplifier. (b) Equivalent circuit of class-E amplifier.

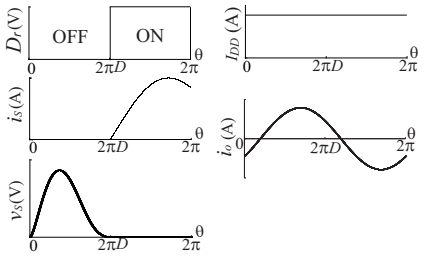

Figure 2: Example waveforms in the class-E power amplifier satisfying nominal conditions for $D = 0.5$.

By carrying out circuit experiments, we can confirm the validity of the distribution maps.

2. Fundamental Switching-Pattern

2.1. Circuit Description and Principle Operation

Figure 1(a) shows the circuit topology of the class-E power amplifier [1]-[4]. This amplifier is composed of a dc-supply voltage source V_{DD}, a dc-feed inductance L_C, a MOSFET as the switching device S, a shunt capacitance C_S, and a series-resonant filter L_0-C_0-R. When the class-E amplifier satisfies the zero-voltage switching (ZVS) and the zero-derivative switching (ZDS) conditions simultaneously at the switch turn-on instant, the class-E amplifier achieves high power-conversion efficiency at high frequencies and low switching noise. These switching conditions are called the class-E ZVS/ZDS conditions or the nominal conditions,

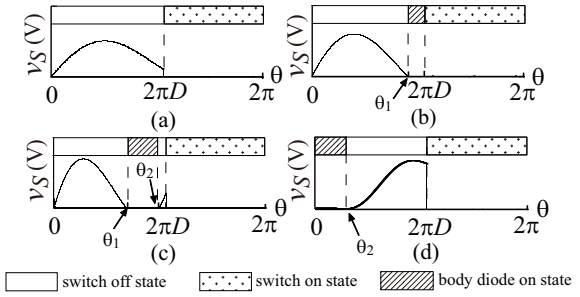

Figure 3: Switching patterns of the class-E amplifier outside nominal operation. (a) Case 1. (b) Case 2. (c) Case 3. (d) Case 4.

which are expressed as

$$v_S(2\pi D) = 0, \quad \left.\frac{dv_S(\theta)}{d\theta}\right|_{\theta=2\pi D} = 0, \tag{1}$$

where v_S is the voltage across the switching device and D is a switch-off duty ratio at the driving signal D_r. The switch turns OFF at $\theta = 0$ and turns ON at $\theta = 2\pi D$ by the driving signal D_r.

Figure 2 depicts example waveforms in the class-E power amplifier under nominal operation for $D = 0.5$. During the switch-off interval, the current through the shunt capacitance i_{C_S} produces the switch voltage v_S. During the switch-on interval, the switch current i_S flows the switch and the switch voltage is zero by assuming zero on-resistance. Generally, the resonant filter has a high quality factor Q. In this case, the output currents i_o is a sinusoidal waveform.

2.2. Switching-Patterns of The Class-E Amplifier

Figure 3 shows the switching patterns of the class-E amplifiers outside nominal operation. Figure 3(a) shows the switch-voltage waveform, which does not reach zero prior to turn-on instant. This switching pattern is called "Case 1" in this paper. Conversely, when the switch voltage reaches zero prior to turn-on switching instant, the MOSFET antiparallel body diode turns ON, as shown Fig. 3(b); this is "Case 2". In Case 2, ZVS is achieved at $\theta = \theta_1$ because of the MOSFET body diode. During the MOSFET body diode is in ON state, the switch current is negative. There is a case that the switch voltage returns to positive at $\theta = \theta_2$ via MOSFET-body-diode ON state, as shown in Fig. 3(c), which is "Case 3". This switching pattern occurs when the switch current becomes positive during the anti-parallel diode is in ON state. Additionally, there is also a case that the MOSFET body diode turns ON at $\theta = 0$ and the switch current returns to positive at $\theta = \theta_3$, as shown in Fig. 3(d), which is "Case 4".

2.3. Bifurcation Conditions

A switching pattern changes another one when the switch voltage-waveform equation and/or switch current-waveform equation satisfy certain conditions. The transitions of switching patterns are regarded as bifurcation phenomena. So, switching-pattern transition conditions are expressed as the bifurcation conditions. For the transition of the switching pattern, two types of bifurcation phenomena appear, namely, "border-collision bifurcation" and "grazing bifurcation" [5]. The border-collision bifurcation occurs when a periodic orbit crosses a border. The grazing bifurcation occurs when a part of a orbit tangentially hits a border.

Figure 4 shows the switching-pattern transitions and the switch voltage and the switch current waveforms, which achieve the transition conditions. The transition conditions of the switching patterns are given as follows.

1) Case 1 ↔ Case 2 : This transition occurs when the steady-state switch-voltage-waveform equation in Case 1 satisfies

$$v_{S1}(2\pi D) = 0. \tag{2}$$

where $v_{S1}(\theta)$ is the switch voltage in the switch-off state. This condition means that the switch-voltage waveform crosses the horizontal line at turn-on instant. Therefore, this bifurcation is the border-collision bifurcation.

2) Case 1 ↔ Case 3 : This transition occurs when the steady-state switch-voltage waveform equation in Case 1 satisfies

$$v_{S1}(\theta_1) = 0, \quad \left.\frac{dv_{S1}(\theta)}{d\theta}\right|_{\theta=\theta_1} = 0. \tag{3}$$

This condition means that the switch-voltage waveform grazes the horizontal line. So, this bifurcation is the grazing bifurcation.

3) Case 1 ↔ Case 4 : This transition occurs when the steady-state switch-current-waveform equation in Case 1 satisfies

$$i_S(2\pi) = 0, \quad \left.\frac{di_S(\theta)}{d\theta}\right|_{\theta=2\pi} > 0. \tag{4}$$

It is seen that this bifurcation is the border-collision bifurcation.

4) Case 2 ↔ Case 3 : This transition occurs when the steady-state switch-current-waveform equation in Case 2 satisfies

$$i_S(2\pi D) = 0. \tag{5}$$

This condition means that the switch-current waveform collides the horizontal line at turn off instant. This bifurcation is the border-collision bifurcation.

5) Case 3 ↔ Case 4 : This transition occurs when the steady-state switch-current-waveform equation in Case 4 satisfies

$$i_S(2\pi) = 0, \quad \left.\frac{di_S(\theta)}{d\theta}\right|_{\theta=2\pi} < 0. \tag{6}$$

This bifurcation is the border-collision bifurcation.

3. WAVEFORM EQUATIONS

For obtaining the switching-pattern distributions, we need to derive the waveform equations in the steady state. The analytical steady-state waveform equations for the class-E amplifier are given following the analysis process presented in [2].

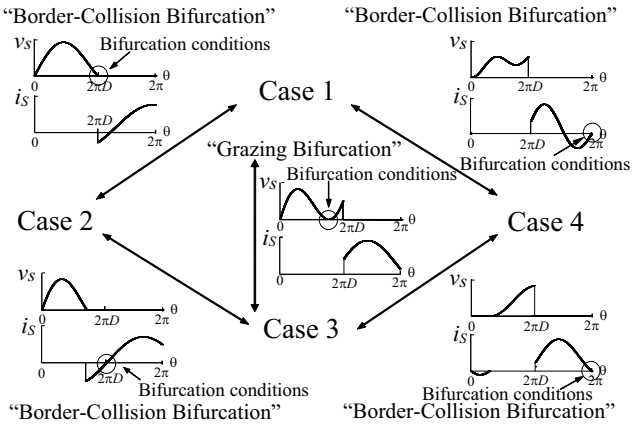

Figure 4: Diagram of switching-pattern bifurcations and examples of waveforms of the switch voltage and the current through the shunt capacitor on each bifurcation conditions.

3.1. Assumptions and Parameters

Figure 1(a) shows a circuit topology of the class-E amplifier. First, we define the following normalized parameters: $A = f_0/f = \omega_0/\omega = 1/\omega\sqrt{L_0C_0}$, $B = C_0/C_S$, $Q = \omega L_0/R$. Additionally, the circuit analysis in this paper is based on the following assumptions:
1) Both the MOSFET and the MOSFET bosy siode act as ideal switch devices.
2) The dc-feed inductance L_C is constant, which is expressed as $i_C = I_{DD}$.

By the above assumptions, the equivalent circuit is obtained, as shown in Fig. 1(b).

3.2. Waveform Equations

From the assumptions and Fig. 1(b), the circuit equations can be formulated. When the switch is OFF, the circuit equations are

$$\begin{cases} \dfrac{1}{RI_{DD}}\dfrac{dv_{S1}(\theta)}{d\theta} = A^2BQ\left(1-\dfrac{i_{o1}(\theta)}{I_{DD}}\right) \\ \dfrac{1}{I_{DD}}\dfrac{di_{o1}(\theta)}{d\theta} = \dfrac{1}{Q}\left(\dfrac{v_{S1}(\theta)}{RI_{DD}} - \dfrac{v_{C1}(\theta)}{RI_{DD}} - \dfrac{i_{o1}(\theta)}{I_{DD}}\right) \\ \dfrac{1}{RI_{DD}}\dfrac{dv_{C1}(\theta)}{d\theta} = A^2Q\dfrac{i_{o1}(\theta)}{I_{DD}}. \end{cases} \tag{7}$$

When the switch or the MOSFET body diode is ON, we have

$$\begin{cases} \dfrac{v_{S2}(\theta)}{RI_{DD}} = 0 \\ \dfrac{1}{I_{DD}}\dfrac{di_{o2}(\theta)}{d\theta} = -\dfrac{1}{QRI_{DD}}\left(\dfrac{v_{C2}(\theta)}{RI_{DD}} + \dfrac{i_{o2}(\theta)}{I_{DD}}\right) \\ \dfrac{1}{RI_{DD}}\dfrac{dv_{C2}(\theta)}{d\theta} = A^2Q\dfrac{i_{o2}(\theta)}{I_{DD}}. \end{cases} \tag{8}$$

Additionally, the switch current during the switch-ON state is

$$\frac{i_S(\theta)}{I_{DD}} = \begin{cases} 0, & \text{for switch OFF} \\ 1-\dfrac{i_{o2}(\theta)}{I_{DD}}, & \text{for switch or body diode ON} \end{cases} \tag{9}$$

From the above circuit equations, the analytical waveform equations in each switch state can be obtained analytically from (A. 1)-(A. 12) in [2].

Waveform equations of the switch ON and OFF states are connected by

$$\begin{gathered} i_{o1}(0) = i_{o2}(2\pi),\ \ i_{o1}(\theta_1) = i_{o2}(\theta_1),\ \ i_{o2}(\theta_2) = i_{o1}(\theta_2), \\ i_{o1}(2\pi D) = i_{o2}(2\pi D),\ \ v_{C1}(0) = v_{C2}(2\pi),\ \ v_{C1}(\theta_1) = v_{C2}(\theta_1), \\ v_{C2}(\theta_2) = v_{C1}(\theta_2),\ \ v_{C1}(2\pi D) = v_{C2}(2\pi D), \\ v_{S1}(0) = v_{S1}(\theta_1) = v_{S1}(\theta_2) = 0. \end{gathered} \tag{10}$$

By solving (10), the analytical expressions of steady-state waveforms for Case 3 can be obtained. The steady-state waveforms of Case 3 can express all the switching patterns. Because the dc-voltage drop across the dc-feed inductor L_C is zero, I_{DD} is expressed analytically as a function of V_{DD} by solving

$$\frac{V_{DD}}{RI_{DD}} = \frac{1}{2\pi}\int_0^{2\pi}\frac{v_S(\theta)}{RI_{DD}}. \tag{11}$$

4. SWITCHING-PATTERN DISTRIBUTION

4.1. Design Parameters

The design specifications for the nominal operation were given as switch-off duty ratio $D = 0.5$ and loaded quality factor $Q = 10$. First, we carry out the design of the class-E amplifier for the class-E ZVS/ZDS conditions by following the designed method presented in [2]. The design parameters are obtained as $A = 0.937$ and $B = 0.575$. Figure 6(a) shows the theoretical waveforms for the nominal conditions. It is seen from Fig. 6(a) that the class-E ZVS/ZDS conditions were achieved in this state.

4.2. Switching-pattern Distribution

By using the transition conditions and the analytical expressions for the steady-state waveforms in the previous section, the switching-pattern transition points can be calculated. By following the bifurcation curves, we can obtain the switching-pattern distributions.

Figure 5(a) shows the switching-pattern distribution on the f/f_{nom}-$C_S/C_{S\,nom}$ plane where the subscription "nom" means the parameter value in nominal conditions. It is obviously seen that three bifurcation conditions in (2), (3) and (6) are achieved simultaneously at the nominal conditions. Additionally, it is also seen that ZVS region, namely Case 2 region, appears only for $f/f_{nom} > 1.0$ and there is no ZVS region for $C_S/C_{S\,nom} > 1.05$.

Figure 5(b) shows the switching-pattern distribution on the f/f_{nom}-D plane. It is seen from Fig. 5(b) that the bifurcation curves in (2) and (3) depict the circle and there are two points that three bifurcation curves of (2), (3) and (6) cross. Therefore, there are two parameter sets, which satisfy the class-E ZVS/ZDS conditions in f/f_{nom}-D plane. Additionally, it is also seen that the Case 2 region appears

Table 1: Analytical Predictions and Experimental Measurements for Nominal Condition

	Analytical	Measured	Difference
D	0.5	0.5	0.00 %
Q	10	10	0.00 %
V_{DD}	5.0 V	5.0 V	0.00 %
f_{nom}	1 MHz	1 MHz	0.00 %
R	5.00 Ω	4.99 Ω	−0.20 %
L_C	34.7 μH	43.0 μH	24.1 %
L_0	7.96 μH	8.01 μH	0.62 %
$C_{S\,nom}$	6.30 nF	6.28 nF	−0.32 %
C_0	3.62 nF	3.60 nF	−0.55 %
A	0.937	0.937	0.00 %
B	0.575	0.573	−0.35 %
P_o	3.01	2.98	−1.03 %

only for $f/f_{nom} > 1.0$, which is similar to the result in Fig. 5(a).

4.3. Experimental Verifications

For circuit experiments, the design specifications for the nominal operation were given as follows: operating frequency $f_{nom} = 1$ MHz, dc-supply voltage $V_{DD} = 5$ V, output resistor $R = 5\ \Omega$, switch-off duty ratio $D = 0.5$ and the loaded quality factor $Q = 10$. An IRF530 MOSFET device was used in the circuit experiment. Table 1 gives analytical predictions and experimental measurements for the nominal conditions. In this table, all element values were measured by HP4284A LCR impedance meter.

Figure 6 shows the theoretical and experimental waveforms. Each waveform parameters correspond to the marks on Fig. 5. We can confirm that the experimental waveforms agree with the theoretical ones quantitatively. This result denotes the validity of the steady-state waveform equations and the switching-pattern distribution maps.

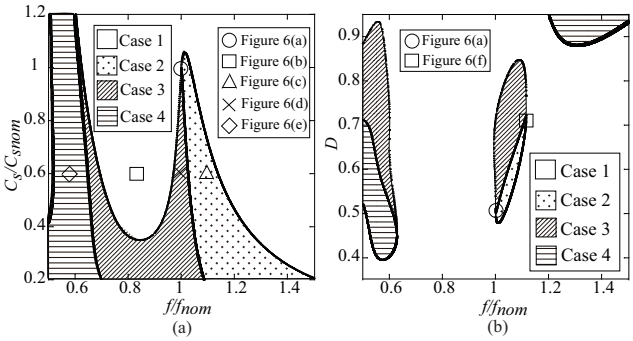

Figure 5: Switching-pattern distributions. (a) f/f_{nom}-$C_S/C_{S\,nom}$ plane. (b) f/f_{nom}-D plane.

5. CONCLUSION

This paper has presented the analytical switching-pattern distributions for the class-E amplifier. The switching patterns are changed via border-collision bifurcation or grazing bifurcation. Therefore, the switching-pattern distribution maps can be obtained for wide parameter region by solving the bifurcation conditions with analytical steady-state waveform expressions and following the bifurcation curves. By carrying out circuit experiments, we can confirm the validity of the distribution maps.

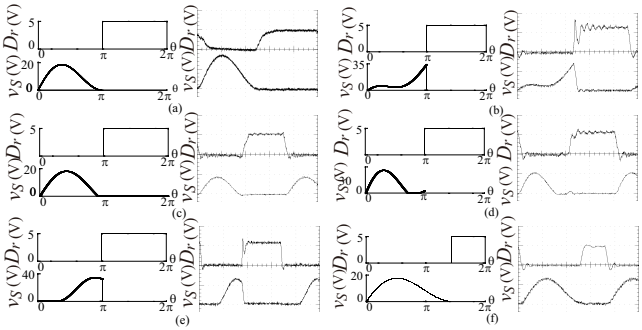

Figure 6: Theoretical and Experimental waveforms. (a) nominal conditions, vertical of v_g: 5 V/div, v_S: 10 V/div. horizontal: 200 ns/div. (b) Case 1, vertical of v_g: 5 V/div, v_S: 20 V/div. horizontal: 250 ns/div. (c) Case 2, vertical of v_g: 5 V/div, v_S: 10 V/div. horizontal: 200 ns/div. (d) Case 3, vertical of v_g: 5 V/div, v_S: 20 V/div. horizontal: 250 ns/div. (e) Case 4, vertical of v_g: 5 V/div, v_S: 20 V/div. horizontal: 500 ns/div. (f) Class-E switching, vertical of v_g: 5 V/div, v_S: 10 V/div. horizontal: 250 ns/div.

Acknowledgments

This research was partially supported by Scholarship Foundation and Grant-in-Aid for scientific research (No. 23760253) of JSPS, SCAT, and TAF, Japan.

References

[1] N. O. Sokal and A. D. Sokal, “Class E - A new class of high-efficiency tuned single-ended switching power amplifiers,” *IEEE Jounal of Solid State Circuits*, vol. 10, no. 3, pp. 168–176, Jun. 1975.

[2] M. Albulet and R. E. Zulinski, “Effect of switch duty ratio on the performance of class E amplifiers and frequency multipliers, ” *IEEE Trans. Circuits Syst.*, vol. 45, no. 4, pp. 325–335, Apr. 1998.

[3] T. Suetsugu and M. Kazimierczuk, “Steady-state behavior of class E amplifier outside designed conditions, ” *in Proc. IEEE ISCAS*, Kobe, Japan, May, 2005, pp. 708–711.

[4] T. Nagashima, X. Wei, H. Sekiya, and M. K. Kazimierczuk, “Power conversion efficiency of class-E power amplifier outside nominal operations,” *in Proc. IEEE ISCAS*, Rio de Janeiro, Brazil, May 2011, pp.749–752.

[5] M. di Bernardo, C. J. Budd and A. R. Champneys, “Grazing and border-collision in peacewise-smooth systems: a unified analytical framework,” *Phys. Rev. Lett.*, vol. 86, no. 12, pp. 2553–2556, Mar 2001.